NOTE **Communicated by Arjen van Ooyen**

A Theoretical Model of Axon Guidance by the Robo Code

Geoffrey J. Goodhill
geoff@georgetown.edu
Department of Neuroscience, Georgetown University Medical Center, Washington, D.C. 20007, U.S.A.

After crossing the midline, different populations of commissural axons in *Drosophila* target specific longitudinal pathways at different distances from the midline. It has recently been shown that this choice of lateral position is governed by the particular combination of Robo receptors expressed by these axons, presumably in response to a gradient of Slit released by the midline. Here we propose a simple theoretical model of this combinatorial coding scheme. The principal results of the model are that purely quantitative rather than qualitative differences between the different Robo receptors are sufficient to account for the effects observed following removal or ectopic expression of specific Robo receptors, and that the steepness of the Slit gradient in vivo must exceed a certain minimum for the results observed experimentally to be consistent.

1 Introduction

A crucial process in the construction of a nervous system is the establishment of appropriate connectivity. This consists of two stages: the guidance of axons to target regions largely independent of neural activity, followed by the activity-dependent refinement of synaptic connections. Much progress has recently been made in understanding the mechanisms of axon guidance in response to molecular cues in the developing nervous system (Tessier-Lavigne & Goodman, 1996; Mueller, 1999; Wilkinson, 2001; Song & Poo, 2001). An emerging theme is that a limited number of evolutionarily conserved axon guidance molecules are reused in many different contexts. When it is necessary to generate several different outcomes in the same region of space and time, an obvious strategy is combinatorial coding. For instance, two guidance molecules could simultaneously attract three populations of axons to different targets if population 1 expressed only one type of receptor, population 2 expressed only the other type, and population 3 expressed both types. Since axons can also be attracted or repelled depending on their internal state (Song, Ming, & Poo, 1997), for N guidance molecules, the number of separate populations that could in principle simultaneously be guided to different locations is of order 3^N. About 100 guidance molecules are now known, allowing many more potential outcomes than there are total

connections in any biological nervous system. Combinatorial coding is thus a very efficient coding strategy and is used by nervous systems in contexts ranging from axon guidance (Shirasaki & Pfaff, 2002) to information coding by spike trains (Diesman, Gewaltig, & Aertsen, 1999) and odor coding in the olfactory system (Malnic, Hirono, Sato, & Buck, 1999).

A particularly well-studied model system in axon guidance is the growth of commissural axons to, across, and beyond the midline (Kaprielian, Imondi, & Runko, 2000). Commissural axons are initially attracted toward the midline (e.g., the insect nerve cord or the vertebrate spinal cord) by a gradient of Netrin released by midline glia (Serafini et al., 1994; Kennedy, Serafini, de la Torre, & Tessier-Lavigne, 1994; Mitchell et al., 1996). On reaching the midline, they lose their responsiveness to Netrin but become responsive instead to the repellent molecule Slit, which binds to the Robo family of receptors (Brose et al., 1999; Kidd, Bland, & Goodman, 1999). In *Drosophila*, this currently consists of the three members Robo, Robo2, and Robo3, each of which plays a particular role in enabling commissural axons to cross the midline and not then recross (Rajagopalan, Nicolas, Vivancos, Berger, & Dickson, 2000; Simpson, Kidd, Bland, & Goodman, 2000). After crossing, axons project to specific lateral pathways before turning longitudinally. Recent results from *Drosophila* (Rajagopalan, Vivancos, Nicolas, & Dickson, 2000; Simpson, Bland, Fetter, & Goodman, 2000) have focused on three specific longitudinal Fas-II positive tracts, referred to as medial, intermediate, and lateral. In this case, the choice of pathway depends on a combinatorial code of Robo receptors expressed by axons after they have crossed the midline—the so-called Robo code. Axons that normally turn in the medial tract express only Robo, axons that normally turn in the intermediate tract express Robo and Robo3, and axons that normally turn in the lateral tract express Robo, Robo2, and Robo3 (see Figure 1A). Although a gradient of Slit emanating from the midline has not yet been directly observed, it has been hypothesized that this gradient drives axons to specific lateral positions based on their combinatorial code of Robo receptors (Rajagopalan, Vivancos, Nicolas, & Dickson, 2000; Simpson, Bland, Fetter, & Goodman, 2000). This hypothesis is supported by loss- and gain-of-function experiments (Rajagopalan, Vivancos, Nicolas, & Dickson, 2000; Simpson, Bland, Fetter, & Goodman, 2000). When particular Robo receptors are deleted, axons often project to a more medial fascicle than normal, whereas when particular Robo receptors are ectopically expressed, axons often project to a more lateral fascicle than normal. The shifts induced by these genetic perturbations are always discrete jumps between fascicles: these axons do not generally turn between fascicles. Both Rajagopalan, Vivancos, Nicolas, and Dickson (2000) and Simpson, Bland, Fetter, and Goodman, (2000) argue that the Robo code targets axons to a general region; then local cues take over to target a particular tract within that region.

Although these different Robo receptors all mediate repulsion by Slit, the specific signal transduction pathways they activate inside the growth

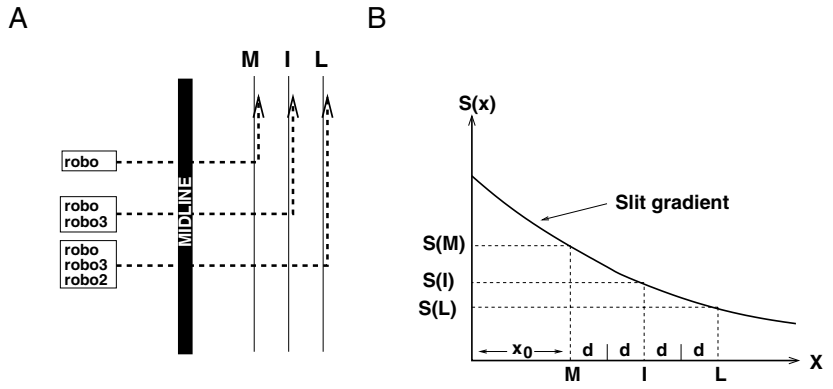

Figure 1: (A) Schematic diagram of the Robo code. Three different populations of commissural axons (dashed lines) are shown projecting to three different lateral fascicles: M (medial), I (intermediate), and L (lateral). (B) Parameters of the model. x_0 = distance of the medial fascicle from the midline, $2d$ = spacing of the fascicles. S(M), S(I), and S(L) refer to the Slit concentrations at the medial, intermediate, and lateral fascicles, respectively.

cone may be different (discussed in Rajagopalan, Vivancos, Nicolas, & Dickson, 2000). One possibility is that each type of Robo receptor signals qualitatively different information regarding levels of Slit, which would be a combinatorial code in the sense most analogous to the other examples cited above. However, an alternative possibility is that the differences between types of Robo receptors are simply quantitative; each generates the same type of repulsive signal to particular levels of Slit, differing only in degree. Roughly speaking, this is consistent with the experimental results that the more Robo receptors an axon expresses, the more repulsion and thus the further its lateral projection. By analogy with levels of measurement in statistics (Krzanowski, 1988), we refer to the first possibility as a categorical model and the second as a ratio model. In the categorical model, only the categories of Robo receptors expressed by a given axon determine where it projects to, whereas in the ratio model, only the relative proportions matter. The categorical model is consistent with many of the experimental results. For instance, overexpressing Robo does not generally cause a lateral shift (Simpson, Bland, Fetter, & Goodman, 2000). However, a purely categorical model is insufficient to explain some results: for instance, axons that normally project laterally still do so in the *robo/robo3* double mutant (Simpson, Bland, Fetter, & Goodman, 2000), and medially projecting axons that project to the intermediate zone when *robo3* is added can be "supershifted" to the lateral zone by the addition of two copies of the robo3 gene (Rajagopalan, Vivancos, Nicolas, & Dickson, 2000). Results such as these led both Simpson, Bland, Fetter, and Goodman (2000) and Rajagopalan, Vi-

vancos, Nicolas, and Dickson (2000) to propose a mixed categorical-ratio model, where Robo acts as a category (only the presence of Robo is important, not its precise amount) and Robo2 and Robo3 act in a more graded way.

To explore these coding issues in a more quantitative way, we have developed a simple mathematical model of the Robo code based on a pure ratio and a mixed categorical-ratio approach. We show that a pure ratio model could in fact be consistent with the data if the Slit gradient is steep enough. This leads to experimentally testable predictions regarding how the outcome of Robo overexpression experiments might depend on the steepness of the Slit gradient. In addition, for the mixed categorical-ratio model, we show that even this version is consistent with the data only when the Slit gradient is sufficiently steep.

2 Mathematical Model

2.1 Form of the Slit Gradient. There is no direct evidence concerning the shape of the Slit gradient in vivo. Theoretically, one approach would be to model it as free diffusion from a line source in an infinite three-dimensional volume (Crank, 1975; Carslaw & Jaeger, 1959), analogous to a recent model of axon guidance by a target-derived diffusible factor (Goodhill, 1997, 1998). However, data from other systems suggest the diffusion might not be free (Hiramoto, Hiromi, Giniger, & Hotta, 2000). Given this uncertainty, it seems sensible to choose a very generic shape with a parameterized steepness for the Slit gradient. We therefore assume it to be a decaying exponential, $S(x) = Ce^{-x/\alpha}$, where C gives the concentration of Slit at the midline, x is distance from the midline, and α gives the rate of decrease moving away from the midline. For small α, Slit is tightly concentrated around the midline, whereas for larger α, it decays more gradually.

2.2 Generation of Repulsion: Linear Model. In the linear version of the model, we assume that the amount of repulsion induced in growth cones by Slit is given by $S(x) \times R$, where R is just a sum of the amount of repulsion transduced by each Robo receptor separately (Nakamoto et al., 1996; Goodhill & Richards, 1999). That is, $R = r$ for axons normally projecting to the medial fascicle, $R = r + r_3$ for intermediate axons, and $R = r + r_3 + r_2$ for lateral axons, where r, r_3, and r_2 give the "net" amount of repulsion due to each Robo receptor (for the mixed categorical-ratio model, R is assumed to depend on only r_2 and r_3). The values of the r's that are consistent with the data come out of the model. For experiments where a second copy of a gene is inserted, this net repulsion is assumed to be doubled. That is, the net repulsion is assumed to be equal to the product of the number of receptors times the strength of repulsive signaling through a single receptor of that type. For Robo overexpression experiments, where the degree of amplification of r is uncertain, we introduce a multiplication

parameter n. The values of n that are consistent with the data emerge from the model.

Each axon is assumed to be repelled by Slit until the amount of repulsion $S(x) \times R$ reaches a certain threshold T that is the same for all axons. Axons are then assumed to be attracted by local cues toward the nearest of the medial, intermediate, or lateral fascicles. The model presented here concerns only how axons target a particular general area based on their Robo code and does not explicitly address how local cues refine their positions within these general areas (we return to this in section 4). This means that the positions that axons reach defined purely by Slit repulsion can be anywhere in the region of a particular fascicle, provided they are nearer to that fascicle than neighboring fascicles. Fascicles are assumed to be evenly spaced, distance $2d$ apart, with the medial fascicle distance x_0 from the midline (see Figure 1B). We also assume that for axons to project to the medial fascicle, their turning position must be more than $x_0 - d$ from the midline, and for axons to project to the lateral fascicle, their turning position must be less than $x_0 + 5d$ from the midline. Based on data such as Figure 5A of Simpson, Bland, Fetter, and Goodman (2000), we chose $x_0 = 4, d = 1$ (in arbitrary units), so that the three fascicles run at distances 4, 6, and 8 from the midline (absolute distances are not indicated in Simpson, Bland, Fetter, & Goodman, 2000, or Rajagopalan, Vivancos, Nicolas, & Dickson, 2000). These units set the scale for α.

The constraints imposed by the experimental data can now be expressed as a set of inequalities that must all be simultaneously satisfied. As an example, consider the normal targeting of axons projecting to the intermediate fascicle. The equation for targeting to position x is

$$S(x)(r + r_3) = T. \tag{2.1}$$

Substituting the exponential form for S gives

$$e^{-x/\alpha}(r + r_3) = T/C.$$

The ratio T/C sets the absolute scale for the r's. However, since we are interested only in the relative values of the r's, we can without loss of generality set $T/C = 1$. This yields a value for x of

$$x = \alpha \log(r + r_3). \tag{2.2}$$

This target position must be closer to the intermediate tract than either the medial or lateral tracts. Thus we require (cf. Figure 1) that

$$x_0 + d < \alpha \log(r + r_3) < x_0 + 3d$$

or equivalently

$$e^{\frac{x_0+d}{\alpha}} < r + r_3 < e^{\frac{x_0+3d}{\alpha}}.$$

Table 1 shows a set of inequalities that can be derived by this approach from the experimental data of Rajagopalan, Vivancos, Nicolas, and Dickson (2000) and Simpson, Bland, Fetter, and Goodman (2000) (see particularly the schematic Figure 4 in Simpson, Bland, Fetter, & Goodman, 2000). Cases labeled "crossing defect" are assumed to represent problems with crossing rather than lateral termination zone and are not considered further in our analysis. In case 9 in Table 1 (axons that normally project to the lateral fascicle in the robo2 mutant), the axons seem undecided between the intermediate and lateral fascicles. This was not included in our analysis, and we return to this issue in section 4.

Not all of these inequalities are independent. For instance, if $\alpha \log(r_3) > x_0 + d$ (index 5 in Table 1), then it is certainly true that $\alpha \log(r + r_3) > x_0 + d$ (index 2 in Table 1), and the latter constraint is superfluous. However, we explicitly include all the constraints in Table 1 since it makes it easier to see which piece of datum each is based on and what would happen if each were deleted or altered.

2.3 Generation of Repulsion: Nonlinear Model. A more realistic picture of binding kinetics than the linear version presented above is

$$[RL] = \frac{[R][L]}{[L] + K_d},$$

where $[R]$ is the receptor concentration, $[L]$ is the ligand concentration, $[RL]$ is the concentration of the product, and K_d is the dissociation constant (Gutfreund, 1995). When $[L] \ll K_d$, this simplifies to the linear version (with K_d absorbed into the threshold T). The three Robo receptors have similar K_ds for binding Slit, in the range 10 to 40 nM (Simpson, Kidd, Bland, & Goodman, 2000), and we consider these as equal. The analog of equation 2.1 is then

$$\frac{S(x)}{S(x) + K_d}(r + r_3) = T.$$

Substituting the exponential form for $S(x)$ and dividing by C gives

$$\frac{e^{-x/\alpha}}{e^{-x/\alpha} + 1/\bar{c}}(r + r_3) = T, \tag{2.3}$$

where $\bar{c} = C/K_d$, the normalized Slit concentration at the midline. Again, T simply sets the overall scale of the r's, so we can set it to 1 without loss of generality. The analog to equation 2.2 is now

$$x = \alpha \log[\bar{c}(r + r_3 - 1)],$$

and an analogous set of constraints to Table 1 can be generated (not shown).

Table 1: Complete Set of Constraints for the Linear Model Derived from Wild Type and Mutants.

Index	Mutant	Population	Robo Code			Equation		
1	WT	Medial	r	$x_0 - d$	$<$	$\alpha \log(r)$	$<$	$x_0 + d$
2	WT	Intermediate	r, r_3	$x_0 + d$	$<$	$\alpha \log(r + r_3)$	$<$	$x_0 + 3d$
3	WT	Lateral	r, r_3, r_2	$x_0 + 3d$	$<$	$\alpha \log(r + r_2 + r_3)$	$<$	$x_0 + 5d$
4	$r-$	Medial				Crossing defect		
5	$r-$	Intermediate	r_3	$x_0 + d$	$<$	$\alpha \log(r_3)$	$<$	$x_0 + 3d$
6	$r-$	Lateral	r_2, r_3	$x_0 + 3d$	$<$	$\alpha \log(r_2 + r_3)$	$<$	$x_0 + 5d$
7	r_2-	Medial	r	$x_0 - d$	$<$	$\alpha log(r)$	$<$	$x_0 + d$
8	r_2-	Intermediate	r, r_3	$x_0 + d$	$<$	$\alpha \log(r + r_3)$	$<$	$x_0 + 3d$
9	r_2-	Lateral	r, r_3			See text		
10	r_3-	Medial	r	$x_0 - d$	$<$	$\alpha \log(r)$	$<$	$x_0 + d$
11	r_3-	Intermediate	r	$x_0 - d$	$<$	$\alpha \log(r)$	$<$	$x_0 + d$
12	r_3-	Lateral	r, r_2	$x_0 + 3d$	$<$	$\alpha \log(r + r_2)$	$<$	$x_0 + 5d$
13	$r-, r_2-$	Medial				Crossing defect		
14	$r-, r_2-$	Intermediate	r_3			Crossing defect		
15	$r-, r_2-$	Lateral	r_3			Crossing defect		
16	$r-, r_3-$	Medial				Crossing defect		
17	$r-, r_3-$	Intermediate				Crossing defect		
18	$r-, r_3-$	Lateral	r_2	$x_0 + 3d$	$<$	$\alpha \log(r_2)$	$<$	$x_0 + 5d$
19	r_2-, r_3-	Medial	r	$x_0 - -d$	$<$	$\alpha \log(r)$	$<$	$x_0 + d$
20	r_2-, r_3-	Intermediate	r	$x_0 - -d$	$<$	$\alpha \log(r)$	$<$	$x_0 + d$
21	r_2-, r_3-	Lateral	r	$x_0 - d$	$<$	$\alpha \log(r)$	$<$	$x_0 + d$
22	nr	Medial	nr	$x_0 - d$	$<$	$\alpha \log(nr)$	$<$	$x_0 + d$
23	nr	Intermediate	nr, r_3	$x_0 + d$	$<$	$\alpha \log(nr + r_3)$	$<$	$x_0 + 3d$
24	nr	Lateral	nr, r_3, r_2	$x_0 + 3d$	$<$	$\alpha \log(nr + r_3 + r_2)$	$<$	$x_0 + 5d$
25	r_2+	Medial	r, r_2	$x_0 + 3d$	$<$	$\alpha \log(r + r_2)$	$<$	$x_0 + 5d$
26	r_3+	Medial	r, r_3	$x_0 + d$	$<$	$\alpha \log(r + r_3)$	$<$	$x_0 + 3d$
27	r_2+, r_3+	Medial	r, r_3, r_2	$x_0 + 3d$	$<$	$\alpha \log(r + r_3 + r_2)$	$<$	$x_0 + 5d$
28	$2r_3+$	Medial	$r, 2r_3$	$x_0 + 3d$	$<$	$\alpha \log(r + 2r_3)$	$<$	$x_0 + 5d$
29	$2r_2+, r_3+$	Medial	$r, r_3, 2r_2$	$x_0 + 3d$	$<$	$\alpha \log(r + r_3 + 2r_2)$	$<$	$x_0 + 5d$

Notes: $r-$ indicates null mutant for Robo and so on; r_2+ indicates ectopic expression for Robo2 and so on; $2r_2$ indicates two copies of Robo2. "Population" identifies the axons involved in each case by where they would normally project to in the wild type (WT).

3 Results

3.1 Linear Model. In the mixed categorical-ratio model, it is assumed that only r_2 and r_3 act in a quantitative way: the set of constraints used is as in Table 1, except that r is ignored (i.e., set to zero). For instance, constraint 2 now becomes $x_0 + d < \alpha \log(r_3) < x_0 + 3d$ (or $e^{(x_0+d)/\alpha} < r_3 < e^{(x_0+3d)/\alpha}$). Since there are now only two variables, r_2 and r_3, each constraint can be represented as a straight line in the r_2, r_3 plane. Figure 2 shows how the constraints conspire to limit the allowable combinations of r_2 and r_3 that satisfy the inequalities. This is illustrated for two gradient steepnesses, $\alpha = 1$ and $\alpha = 2$. It is immediately obvious from Figure 2 that for $\alpha \gtrsim 2$, there can be no more solutions.

For the pure ratio model, there are the additional parameters r and n, giving four dimensions in total, which is hard to represent graphically. To investigate which sets $\{\alpha, r, r_2, r_3\}$ satisfy all the inequalities, an exhaustive search was performed over the parameter space $r_i \in [0, r_{\max}]$ in increments r_{inc} for various values of α. For certain values of α, we found many different combinations of r, r_3, and r_2, which satisfy the constraints. The precise number of solutions per value of α depends on r_{inc}, which was varied for different α. The total number of solutions is not important here, providing solutions exist, but we ensured that there were always at least 100 so that averaging over them would be meaningful. Since only the ratios of the r's are of interest, they were normalized by r_3. The results are shown in Table 2. Means and standard deviations for the r's are quoted: the standard deviations give a measure of the size of the box in the four-dimensional space in which the solutions exist. Several trends are apparent:

- As for the mixed categorical-ratio model, there are no solutions for $\alpha \gtrsim 2$.
- The values of the r's (i.e., the relative strength of signaling of the different Robo receptors) are always ordered $r_2 > r_3 > r$.
- The ratios of the r values become more extreme as α decreases (i.e., the gradient becomes steeper). For instance, for $n = 2$, the ratios r:r_3:r_2 go from 0.4:1:2.2 for $\alpha = 2.0$ to 0.007:1:20.1 for $\alpha = 0.5$.
- For a very steep gradient ($\alpha = 0.5$), values of n (the amplification factor for Robo overexpression experiments) up to 25 are allowable. As α decreases further, even larger values of n are allowed (results not shown). As the gradient becomes shallower, n becomes more restricted, until finally for $\alpha = 2$, solutions exist only for $n = 2$.

3.2 Nonlinear Model. Comparing equations 2.2 and 2.3, it can be seen that the nonlinear model with $S(x) = e^{-x/\alpha}$ is formally equivalent to a linear model with $S(x) = \frac{e^{-x/\alpha}}{e^{-x/\alpha}+1/c}$. Thus, we may think of the nonlinear version

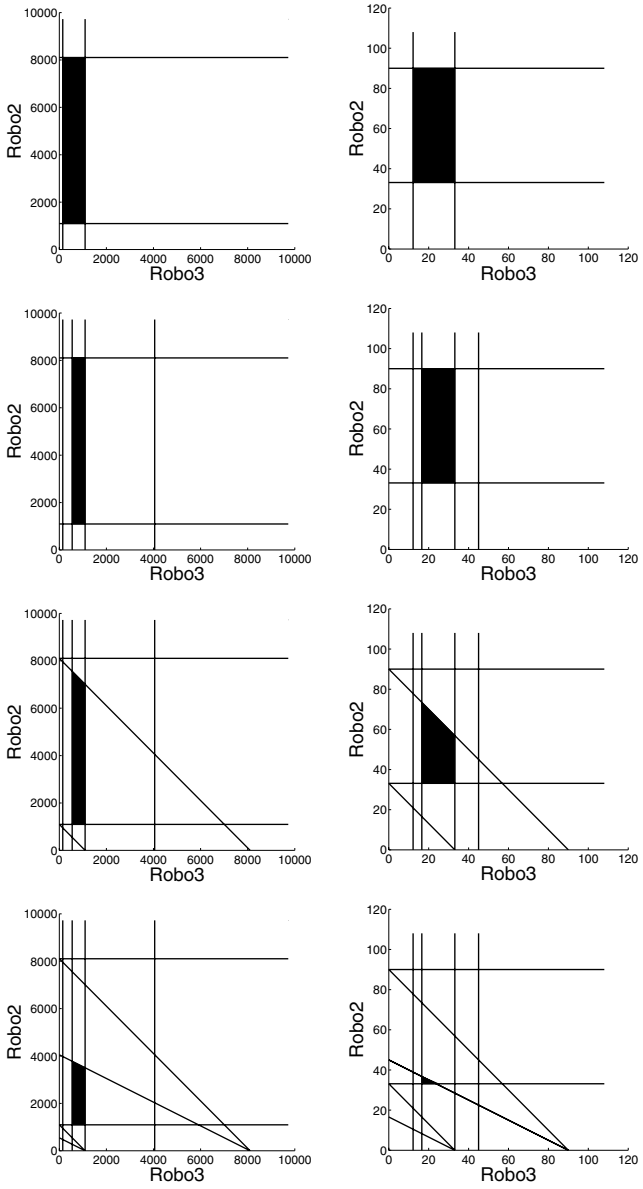

Figure 2: Interaction of constraints for the mixed categorical-ratio model (linear version). (Left) $\alpha = 1.0$. (Right) $\alpha = 2.0$ ($x_0 = 4$, $d = 1$). The shaded box in each case represents the region of r_2–r_3 space allowed by the constraints. First row: cases 2 and 12 from Table 1. Second row: case 28 is added. Third row: case 6 is added. Fourth row: case 29 is added. It can be seen that the allowable region of space shrinks as α increases (the Slit gradient becomes shallower).

Table 2: Values of r, r_2, and r_3 Obtained for the Pure Ratio Model (Linear Version).

n	$\alpha = 0.5$	$\alpha = 1.0$	$\alpha = 2.0$
2	0.0067 ± 0.0038	0.065 ± 0.026	0.35 ± 0.04
	20 ± 11	3.3 ± 1.2	2.2 ± 0.2
3	0.0047 ± 0.0026	0.048 ± 0.015	No solutions
	20 ± 11	3.3 ± 1.2	
4	0.0035 ± 0.0018	0.039 ± 0.010	No solutions
	20 ± 11	3.3 ± 1.2	
5	0.0030 ± 0.0015	0.035 ± 0.007	No solutions
	20 ± 11	3.3 ± 1.2	
6	0.0025 ± 0.0011	0.031 ± 0.005	No solutions
	20 ± 11	3.3 ± 1.2	
7	0.0021 ± 0.0008	No solutions	No solutions
	20 ± 11		
10	0.0017 ± 0.0007	No solutions	No solutions
	20 ± 11		
25	0.001 ± 0.0002	No solutions	No solutions
	20 ± 11		
30	No solutions	No solutions	No solutions

Notes: n is the increase in repulsion compared to wild type in Robo ectopic expression experiments; α is the steepness of the Slit gradient. Shown are the mean and standard deviation of the values obtained for r (above) and r_2 (below) normalized by r_3 (i.e., $r_3 = 1$).

as simply the linear model with a different Slit gradient. In comparing different gradients, the overall scaling is unimportant since in the model, we are interested only in the ratio of the r's. Thus, significant differences are expected only between the results for the linear and nonlinear models when the effective gradients have significantly different shapes in the region between $x = 4$ and $x = 8$. For the range of α considered above, this occurs only when $\bar{c} \gg 1$ (see Figure 3). Table 3 shows results for the pure ratio model for $\bar{c} = 100$, that is, a midline Slit concentration $100K_d$ ($\alpha = 1$). This implies Slit concentrations at the medial, intermediate, and lateral fascicles of $65K_d$, $20K_d$, and $3K_d$, respectively (650 nM, 200 nM, and 30 nM for $K_d = 10$ nM). There are slight differences from the linear model, but overall the general trends are the same. The numerical differences are smaller for smaller $\bar{c}$ (data not shown).

4 Discussion

The model presented here is a way of simplifying a varied and complex set of experimental results so as to attempt to extract certain key pieces of quantitative information about the system. A number of biologically relevant conclusions can be drawn. Perhaps the most important of these is that a pure ratio model can be consistent with the data, despite the fact

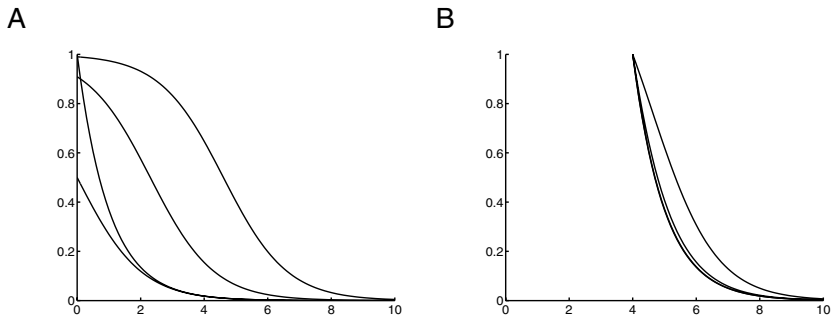

Figure 3: Comparison of an exponential Slit gradient with the effective gradient shape in the nonlinear model. The horizontal axis is distance from the midline; the vertical axis is Slit concentration (arbitrary units). (A) From left to right, effective gradient in nonlinear model for $\bar{c} = 1$, exponential gradient, effective gradient in nonlinear model for $\bar{c} = 10, 100$. (B) Same gradients, but normalized so that the Slit concentration at distance 4 is always 1. From left to right, exponential gradient, effective gradient in nonlinear model for $\bar{c} = 1$ (indistinguishable from exponential), $\bar{c} = 10, 100$. Note that the effective gradient shape diverges significantly from an exponential only when $\bar{c} \gg 1$. For all curves, $\alpha = 1$.

that Simpson, Bland, Fetter, and Goodman (2000) and Rajagopalan, Vivancos, Nicolas, and Dickson (2000) did not generally find lateral shifts when Robo was overexpressed. The model predicts that arbitrarily large degrees of overexpression of Robo may indeed not cause shifts in a ratio model, provided the Slit gradient is sufficiently steep. The reason for this is actually quite intuitive. The ratio of Slit concentration at the intermediate compared to medial fascicles in the linear model is $\frac{e^{-6/\alpha}}{e^{-4/\alpha}} = e^{-2/\alpha}$. As α becomes smaller, this ratio becomes smaller; that is, for steeper gradients, there is a larger disparity between the concentrations at the intermediate and medial fascicles. Since in the linear model the repulsion due to Robo induced by Slit is given by $r \times S(x)$, a larger Slit disparity means that a larger increase in Robo expression is possible before a shift to the intermediate fascicle is induced. Thus, by precisely measuring the actual level of Robo in overexpression experiments where no shifts occur, it should be possible to predict based on the model a minimum steepness for the Slit gradient in vivo. Similarly, the pure ratio model predicts that there should be a certain level of overexpression of Robo at which lateral shifts can be made to occur. Interestingly, Simpson, Bland, Fetter, and Goodman (2000) did in fact find one GAL4 line (15J2) where increased Robo can cause a lateral shift of the dMP2 and vMP2 axons. A possible explanation suggested by the model is that it is only in this line that Robo levels exceed that required for a lateral shift.

A robust result of both the pure ratio and mixed categorical-ratio model is that the experimental data are consistent only when the Slit gradient is

Table 3: Values of r, r_2, and r_3 Obtained for the Pure Ratio Model (Nonlinear Version).

n	$\alpha = 0.5$	$\alpha = 1.0$	$\alpha = 2.0$
2	0.0067 ± 0.0038	0.17 ± 0.028	No solutions
	20 ± 11	3.4 ± 1.2	
3	0.0046 ± 0.0025	No solutions	No solutions
	20 ± 11		
4	0.0036 ± 0.0019	No solutions	No solutions
	20 ± 11		
5	0.0030 ± 0.0015	No solutions	No solutions
	20 ± 11		
6	0.0025 ± 0.0012	No solutions	No solutions
	20 ± 11		
7	0.0022 ± 0.0010	No solutions	No solutions
	20 ± 11		
10	0.0016 ± 0.0007	No solutions	No solutions
	20 ± 11		
25	0.00083 ± 0.00016	No solutions	No solutions
	20 ± 11		
30	0.00083 ± 0.00016	No solutions	No solutions
	20 ± 11		
35	No solutions	No solutions	No solutions

Notes: n is the increase in repulsion compared to wild type in Robo ectopic expression experiments; α is the steepness of the Slit gradient. Shown are the mean and standard deviation of the values obtained for r (above) and r_2 (below) normalized by r_3 (i.e., $r_3 = 1$).

sufficiently steep. For the linear model, the cut-off is about $\alpha \gtrsim 2$. For the nonlinear model, the cut-off depends on $\bar{c}$, the midline concentration compared to K_d. When $\bar{c} \lesssim 1$, the cut-off is similar to the linear model; for higher values of $\bar{c}$, a slightly steeper gradient is required. According to the linear model, the shallowest allowable Slit gradient consistent with the data has a concentration at the medial fascicle (position $x_0 = 4$) of approximately $e^{-4/2} = 0.14$ times its concentration at the midline, and corresponding values 0.05 and 0.03 at the intermediate and lateral fascicles, respectively. The exact numbers are dependent on the assumption of an exponential gradient shape; while there is no direct experimental evidence for this shape, there is no direct evidence for any other shape either. The exponential function provides a convenient way of exploring gradients varying from very steep (small α) to very shallow (large α) and has been used to model the gradient in previous theoretical analyses of axon guidance such as Gierer (1987). When experimental data about Slit gradients in vivo become available, these could be used in the model instead. Although changing the gradient function will likely change the precise numerical results, it is unlikely to have a strong effect on the general conclusions of the model.

What implications does this work have for our understanding of the coding strategies employed in axon guidance? In a strict sense, the pure ratio model is not a combinatorial code, since the receptors are interchangeable with appropriate scaling. In this case, why have three receptors when in principle one would do? One possibility is that more than one receptor type is already required by commissural axons for midline crossing (Rajagolapalan, Vivancos, Nicolas, & Dickson, 2000; Simpson, Bland, Fetter, & Goodman, 2000), and since this diversity is available, it is simply reused. However, an alternative possibility is that it might not be possible to robustly achieve the widely but precisely different levels of expression that would be required of a single receptor. From Table 2, for $\alpha = 0.5$, the relative levels of expression needed for the putative single receptor would be 0.0067 for axons projecting to the medial tract, 1.0067 for axons projecting to the intermediate tract, and 21.0067 for axons projecting to the lateral tract. These differ by a factor of about 3000. Since the number of receptors expressed on the surface of a growth cone is probably no more than about 10,000, the number of receptors present on the growth cones of medially projecting axons would need to be about 3. Even if it was possible to achieve this precisely, the response of these axons to a Slit gradient would then be overwhelmed by noise (Berg & Purcell, 1977; Goodhill & Urbach, 1999). While it is true that for the shallowest gradients allowable by the model, these demands are more reasonable (e.g., for $\alpha = 2.0$, the difference in expression required would be about a factor of ≈ 10), using multiple receptors with different strengths of signaling is clearly a more robust strategy overall.

The model presented here does not consider the precise timing of robo expression, that is, the way the expression of each robo receptor varies as axons traverse the midline and then project laterally. It also does not consider how local cues refine axonal targeting within a general region. One hypothesis is that each specific Fas II tract releases an attractive factor, and it is the balance of this attractive force with the Slit repulsion that guides axons to a specific tract. To include such a mechanism in the model would, however, require introducing additional parameters whose values are not currently constrained by experimental data. Also, there is a general problem with this hypothesis in that such an attractive force would necessarily decay symmetrically on each side of the Fas II tract, whereas the Slit repulsion is asymmetric on each side of the tract. The current model instead remains agnostic about the nature of this local focusing mechanism. The model also does not take into account the fact that many of the mutant and misexpression results listed in Table 1 are in reality just statistical tendencies and do not occur in 100% of cases (this is particularly true in case 9). A possible extension of the model would include probabilistic rules, for instance, that there is noise in the measurement of the level of Slit present (Berg & Purcell, 1977; Goodhill & Urbach 1999).

Although we have shown that qualitative differences between robo receptors are not required to account for the lateral targeting of commis-

sural axons in *Drosophila*, it does not rule out the possibility that qualitative differences play a role. There are several other indications that qualitative differences between Robo and Robo2/Robo3 do exist (Simpson, Kidd, Bland, & Goodman, 2000). *Robo2* and *Robo3* are positioned close by chromosomally and have closely related sequences. Their intracellular capabilities are different from Robo; for instance, unlike Robo, they lack an Enabled binding site. The different Robos certainly play qualitatively different roles in the midline crossing of commissural axons (Simpson, Kidd, Bland, & Goodman, 2000) and in the growth and guidance of motor neuron dendrites (Godenschwege et al., 2002). Rajagopalan, Vivancos, Nicolas, and Dickson (2000) report that experiments are now under way to generate chimeric Robo receptors, where, for example, the extracellular domain of Robo is coupled to the intracellular domain of Robo2. This will give information about the relative importance of the different signal transduction pathways that Robo and Robo2/Robo3 activate. The model we have presented so far combines extra- and intracellular effects into a single effective strength of signaling. An extension would be to split each r value into the product $r^e \times r^i$, representing extra- and intracellular influences, respectively. When available, the chimeric receptor data could then be used to constrain the additional three parameters and determine whether there are any sets of values that are still consistent with a purely quantitative model.

Acknowledgments

I thank the anonymous referees for many helpful suggestions for improving this article.

References

Berg, H. C., & Purcell, E. M. (1977). Physics of chemoreception. *Biophysical Journal, 20*, 193–219.

Brose, K., Bland, K. S., Wang, K. H., Arnott, D., Henzel, W., Goodman, C. S., Tessier-Lavigne, M., & Kidd, T. (1999). Slit proteins bind robo receptors and have an evolutionarily conserved role in repulsive axon guidance. *Cell, 96*, 795–806.

Carslaw, H. S., & Jaeger, J. C. (1959). *Conduction of heat in solids* (2nd ed.). Oxford: Clarendon Press.

Crank, J. (1975). *The mathematics of diffusion* (2nd ed.). Oxford: Clarendon Press.

Diesmann, M., Gewaltig, M. O., & Aertsen, A. (1999). Stable propagation of synchronous spiking in cortical neural networks. *Nature, 402*, 529–533.

Gierer, A. (1987). Directional cues for growing axons forming the retinotectal projection. *Development, 101*, 479–489.

Godenschwege, T. A., Simpson, J. H., Shan, Y., Bashaw, G. J., Goodman, C. S., & Murphey, R. K. (2002). Ectopic expression in the giant fiber system of

Drosophila reveals distinct roles for Rounabout (Robo) Robo2, and Robo3 in dendritic guidance and synaptic connectivity. *J. Neurosci., 22*, 3117–3129.

Goodhill, G. J. (1997). Diffusion in axon guidance. *European Journal of Neuroscience, 9*, 1414–1421.

Goodhill, G. J. (1998). Mathematical guidance for axons. *Trends in Neurosciences, 21*, 226–231.

Goodhill, G. J., & Richards, L. J. (1999). Retinotectal maps: Molecules, models, and misplaced data. *Trends in Neurosciences, 22*, 529–534.

Goodhill, G. J., & Urbach, J. S. (1999). Theoretical analysis of gradient detection by growth cones. *Journal of Neurobiology, 41*, 230–241.

Gutfreund, H. (1995). *Kinetics for the life sciences*. Cambridge: Cambridge University Press.

Hiramoto, M., Hiromi, Y., Giniger, E., & Hotta, Y. (2000). The *Drosophila* Netrin receptor Frazzled guides axons by controlling Netrin distribution. *Nature, 406*, 886–889.

Kaprielian, Z., Imondi, R., & Runko, E. (2000). Axon guidance at the midline of the developing CNS. *Anat. Rec., 261*, 176–197.

Kennedy, T. E., Serafini, T., de la Torre, J. R., & Tessier-Lavigne, M. (1994). Netrins are diffusible chemotropic factors for commissural axons in the embryonic spinal cord. *Cell, 78*, 425–435.

Kidd, T., Bland, K. S., & Goodman, C. S. (1999). Slit is the midline repellent for the robo receptor in *Drosophila*. *Cell, 96*, 785–794.

Krzanowski, W. J. (1988). *Principles of multivariate analysis: A user's perspective*. New York: Oxford University Press.

Malnic, B., Hirono, J., Sato, T., & Buck, L. B. (1999). Combinatorial receptor codes for odors. *Cell, 96*, 713–723.

Mitchell, K. J., Doyle, J. L., Serafini, T., Kennedy, T. E., Tessier-Lavigne, M., Goodman, C. S., & Dickson, B. J. (1996). Genetic analysis of Netrin genes in *Drosophila*: Netrins guide CNS commissural axons and peripheral motor axons. *Neuron, 17*, 203–215.

Mueller, B. K. (1999). Growth cone guidance: First steps towards a deeper understanding. *Annu. Rev. Neurosci., 22*, 351–388.

Nakamoto, M., Cheng H. J., Friedman, G. C., Mclaughlin, T., Hansen, M. J., Yoon, C. H., O'Leary, D. D. M., & Flanagan, J. G. (1996). Topographically specific effects of ELF–1 on retinal axon guidance in–vitro and retinal axon mapping in–vivo. *Cell, 86*, 755–766.

Rajagopalan, S., Nicolas, E., Vivancos, V., Berger, J., & Dickson, B. J. (2000). Crossing the midline: Roles and regulation of Robo receptors. *Neuron, 28*, 767–777.

Rajagopalan, S., Vivancos, V., Nicolas, E., & Dickson, B. J. (2000). Selecting a longitudinal pathway: Robo receptors specify the lateral position of axons in the *Drosophila* CNS. *Cell, 103*, 1033–1045.

Serafini, T., Kennedy, T. E., Galko, M. J., Mirzayan, C., Jessell, T. M., & Tessier-Lavigne, M. (1994). The netrins define a family of axon outgrowth–promoting proteins homologous to *C. elegans* UNC–6. *Cell, 78*, 409–424.

Shirasaki, R., & Pfaff, S. L. (2002). Transcriptional codes and the control of neuronal identity. *Annu. Rev. Neurosci., 25*, 251–281.

Simpson, J. H., Kidd, T., Bland, K. S., & Goodman, C. S. (2000). Short-range and long-range guidance by slit and its Robo receptors: Robo and Robo2 play distinct roles in midline guidance. *Neuron, 28*, 753–766.

Simpson, J. H., Bland, K. S., Fetter, R. D., & Goodman, C. S. (2000). Short range and long range guidance by Slit and its Robo receptors: A combinatorial code of Robo Receptors controls lateral position. *Cell, 103*, 1019–1032.

Song, H., Ming, G. L., & Poo, M.-M. (1997). CAMP-induced switching in turning direction of nerve growth cones. *Nature, 388*, 275–279.

Song, H., & Poo, M.-M. (2001). The cell biology of neuronal navigation. *Nat. Cell. Biol., 3*, E81–88.

Tessier-Lavigne, M., & Goodman, C. S. (1996). The molecular biology of axon guidance. *Science, 274*, 1123–1133.

Wilkinson, D. G. (2001). Multiple roles of Eph receptors and ephrins in neural development. *Nat. Rev. Neurosci., 2*, 155–164.

Received April 25, 2002; accepted August 5, 2002.